contrast, covering as much as 100 Å$^2$, can sometimes be seen; the pattern is such as could result from fringes produced by a crystallite, with a superposed random contrast from another part of the specimen, behind or in front of the crystallite. Considerations set out above make this a much more likely explanation than that the fairly regular pattern observed could all originate from a volume $A't$ of material with a random-network structure.

*Summer visitor from University of Edinburgh, United Kingdom.
[1]S. C. Moss and J. F. Graczyk, Phys. Rev. Lett. **23**, 1167 (1969).
[2]D. Henderson and F. Herman, J. Non-Cryst. Solids **8**, 359 (1972).
[3]N. J. Shevchik, Bull. Am. Phys. Soc. **16**, 347 (1972).
[4]D. E. Polk, J. Non-Cryst. Solids **5**, 365 (1971).
[5]M. L. Rudee and A. Howie, Philos. Mag. **25**, 1001 (1972).
[6]P. Chaudhari, J. F. Graczyk, and S. R. Herd, Phys. Status Solidi B **51**, 801 (1972).
[7]P. Chaudhari, J. F. Graczyk, and H. P. Charbnau, Phys. Rev. Lett. 29, 425 (1972).
[8]P. B. Hirsch, A. Howie, R. B. Nicholson, D. W. Pashley, and M. J. Whelan, *Electron Microscopy of Thin Crystals* (Plenum, New York, 1965).
[9]M. H. Brodsky, D. Kaplan, and J. F. Ziegler, Appl. Phys. Lett. 21, 305 (1972).
[10]A. Klug and R. A. Crowther, Nature (Lond.) **238**, 435 (1972).
[11]A. J. C. Wilson, Acta Crystallogr. **2**, 318 (1949).
[12]Since my return to Edinburgh, I learned that similar calculations have been made for $SiO_2$ by A. Howie, O. Krivanek, and M. Rudee [Philos. Mag. 27, 235 (1973)]. We agree in our general conclusions.

PHYSICAL REVIEW B VOLUME 8, NUMBER 2 15 JULY 1973

# Interaction of Acoustic Waves with Acceptor Holes in Silicon: The Influence of Internal Stress

Takehiko Ishiguro
*Electrotechnical Laboratory, Mukodai, Tanashi, Tokyo 188, Japan*
(Received 22 January 1973)

The temperature and the magnetic field dependences of the ultrasonic attenuation are measured at low temperatures in lightly doped $p$-Si samples with various impurity concentrations and dislocation densities. In the dislocation-free sample, a peak is found in the temperature dependence, which is related to the content of acceptors. In the sample with high dislocation density ($2 \times 10^4$ cm$^{-2}$), an additional attenuation is found below 3 K which is ascribed to the resonance absorption by acceptor holes and the attenuation is quenched with a lower magnetic field (about 10 kG) than that in the dislocation-free sample. It is also found that the stress caused by an In-bonded quartz-plate transducer changes the attenuation remarkably below 3 K. Therefore ZnO piezoelectric thin films were used in the present study. The observations are explained semiquantitatively in terms of the acceptor-hole–lattice interactions in the effective-mass approximation by taking the distribution of the internal stresses into account after Suzuki and Mikoshiba. The apparent difference in the contributions to the attenuation from the correlation among the impurities and from the dislocations is ascribed to the differences in the distribution of the internal stresses. It is pointed out that the degeneracy of the acceptor ground state is lifted even in the samples with boron content of $5 \times 10^{16}$ cm$^{-3}$ because of the electronic correlations among the randomly distributed impurities.

## I. INTRODUCTION

Ultrasonic attenuation at low temperatures in *lightly or heavily* doped $n$-type Si is well explained in terms of the relaxation process of electrons among donor levels or among valleys of the conduction band.[1–7] The change in the elastic modulus in *heavily doped* $p$-type Si is also explained in terms of the coupling between acoustic waves and degenerate hole gas.[8]

Recently, Suzuki and Mikoshiba[9] proposed a model to explain the ultrasonic attenuation in *lightly doped* $p$-Si,[1] in which holes are bound to acceptors at low temperatures. The model is based on the following terms: (a) The coupling between holes and acoustic waves is calculated in the regime of the effective-mass approximation by using the acceptor-hole-lattice coupling Hamiltonian[10] and by assuming that the wave functions of the relevant acceptor states are representable by $s$-like envelope functions. (b) The presence of randomly distributed internal stresses is assumed, which split the fourfold ground levels of the acceptors into Kramers' doublets.[11] To take the internal stresses into the theory in a tractable way, the random local stresses are represented by the nor-

mal stresses in the [111] or its equivalent directions (the ⟨111⟩ family) and the distribution of their magnitude is expressed by a Gaussian (or Lorentzian). The analyses of the experimental results of the temperature, the uniaxial stress, and the magnetic field dependences of the attenuation[1,12,13] have shown that the presence of the internal stresses is essential to explain the attenuation in *lightly doped p*-Si at low temperatures.[9,13]

The purpose of this paper is to clarify to what the internal stresses are related, by measuring the ultrasonic attenuation as functions of the temperature and the magnetic field, in samples with various impurity concentrations and dislocation densities. It is shown in this paper that the internal stresses increase with the concentration of the impurities. The dislocations also induce the internal stresses, but they contribute to the attenuation in a different way. Phenomenologically, the apparent difference in the excess attenuations by acceptor-hole-lattice interactions in the presence of the impurities and in the presence of the dislocations is ascribed to the difference in the distributions of the internal stresses. The more substantial pictures of the internal stresses are shown to be the electronic correlations among the acceptors for the former and the mechanical stress for the latter.

It has been reported that the reproducibility of the attenuation in the lightly doped *p*-Si is rather poor,[13,14] but it has been found that the reproducibility is closely related either to the unexpected strong dependence of the attenuation on the magnetic field (in the use of magnetic film transducers) or the stress caused by bonded transducers (in the use of quartz-plate transducers). In this paper data free from these messy problems are presented which were obtained by means of ZnO piezoelectric-film transducers and by supporting samples carefully so that external stresses do not act.

## II. EXPERIMENTAL

### A. Temperature Dependence

Boron-doped-Si single crystals belonging to the *low-impurity-concentration region* were used as samples. The acceptor content $N_a$ was estimated from the resistivity at room temperature $\rho$(rt).[15]

TABLE I. Sample characteristics. In the description of the crystal growth, CZ and FZ represent the Czochralski and the floating-zone methods, respectively.

| Sample | Si16*LD* | Si16*MD* | Si16*HD* | Si17*LD* | Si18 |
|---|---|---|---|---|---|
| $N_a$ (cm$^{-3}$) | $4.9\times10^{16}$ | $4.5\times10^{16}$ | $4.6\times10^{16}$ | $4.6\times10^{17}$ | $2\times10^{18}$ |
| $\rho$(rt) ($\Omega$cm) | 0.45 | 0.49 | 0.46 | 0.099 | 0.036 |
| $D_d$ (cm$^{-2}$) | <10 | $10^2-10^3$ | $2\times10^4$ | <10 | |
| Crystal growth | CZ | CZ | FZ | CZ | |

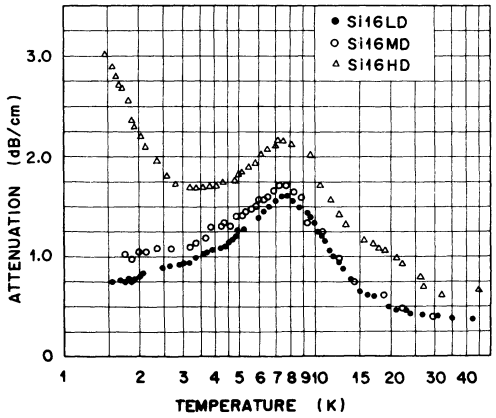


FIG. 1. Temperature dependences of the attenuation of 585-MHz fast transverse waves propagating in the [1$\bar{1}$0] direction for three samples with the same boron content ($4.6-4.9\times10^{16}$ cm$^{-3}$) but with different dislocation densities. In these measurements ZnO-piezoelectric films were used as transducers.

Table I lists $N_a$, $\rho$(rt), dislocation density $D_d$, and the method of crystal growth, which reflects the concentration of oxygen; it is known that pulled Si crystals contain considerable amounts of oxygen as impurities (from $10^{17}$ to $10^{18}$ cm$^{-3}$).[16] This was confirmed in our case also by the presence of the infrared absorption band at 9 $\mu$. Etch-pit density is considered as the dislocation density here. The crystals were kindly supplied by Abe of Shinetsu Semiconductors Co.

The specimens were in the shape of rectangular parallelepipeds about $6\times6\times14$ mm (14 mm along the [1$\bar{1}$0] axis). The ultrasonic waves of 300–600 MHz with the polarization in the [001] direction were propagated along the [1$\bar{1}$0] direction (fast transverse waves). The end faces normal to the propagation direction were polished up to within a parallelism of 5 seconds of arc and a flatness of 600 Å. The transverse waves were generated by means of either sputtered ZnO transducers[17] or In-bonded quartz transducers.

In Fig. 1 are shown the temperature dependences of the attenuation for Si16*LD*, Si16*MD*, and Si16*HD* at 585 MHz obtained by means of ZnO-film transducers. It is remarkable that every sample has an attenuation peak near 8 K whose height is comparable with each of the others, while in Si16*HD* the attenuation increases with decreasing temperature below 3 K in contrast with the cases for Si16*LD* and Si16*MD*. This fact suggests that the character of attenuation peak in the samples with concentration of $5\times10^{16}$ cm$^{-3}$ is related to the content of dopants. On the other hand, the increment below 3 K in Si16*HD* is closely related to the presence of the local stresses due to dislocations.

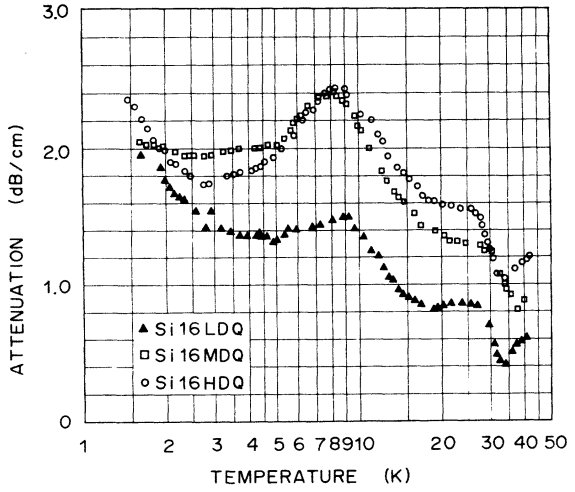


FIG. 2. Temperature dependences of the attenuation of 585-MHz fast transverse waves propagating in the [1$\bar{1}$0] direction. In these measurements, In-bonded quartz plates were used as transducers.

This interpretation of the effect of (mechanical) local stresses due to the presence of the dislocations is supported by the following fact. In the earlier stages of the present work, In-bonded $Y$-cut quartz plates with the thickness of 220 $\mu$ were used as transducers. The reproducibility of the measured attenuation in those days was rather poor for the samples with concentration of $\sim 5\times10^{16}$ cm$^{-3}$; for instance, a rapid cooling of the sample from room temperature to liquid-He region caused bigger attenuations at low temperatures compared with a slow careful cooling. (When a similar cooling process was adopted, however, data were rather reproducible.) In Fig. 2 are shown the temperature dependences of the attenuation which were obtained by means of the quartz-plate transducer. The letter $Q$ added to the name of the sample represents that the measurements were performed with the quartz-plate transducer. Comparing Fig. 1 with Fig. 2, it is found that the two temperature dependences for Si16*HD* and Si16*HDQ* are similar in the sense that the attenuation peaks appearing below 3 K, near 8 K, and near 25 K are observed in both samples, though the peak near 25 K is rather faint in the measurement with the ZnO-film transducers. For the other two dislocation densities, however, the features are different except for the peak near 8 K, and both Si16*LDQ* and Si16*MDQ* are similar to the case for Si16*HD*. This fact clearly indicates that the increment below 3 K is due to the (mechanical) stress caused by the dislocations or by the difference in the thermal expansion coefficients between Si and quartz.[18] A detailed account on this problem will be presented in a separate paper. The temperature dependence of the attenuation of the 400-MHz fast transverse waves in Si17*LD* is shown in Fig. 3, which was obtained by means of the ZnO-film transducer. In this case, the attenuation peak appears around 2 K.

### B. Magnetic Field Dependence

The application of an external magnetic field changes the ground state of the acceptors by causing the Zeeman splitting in addition to the splitting due to the internal stresses. In Figs. 4(a) and 4(b), the dependences of the attenuation on the magnetic field parallel to the [111] direction are shown for Si16*LD* and Si16*HD*, while the magnetic field dependence in Si17*LDQ* has been presented in Ref. 13. These dependences are characterized by the feature that as the magnetic field is increased the attenuation increases first and then decreases down to a saturation level where the excess attenuation due to acceptor-hole-lattice interactions is quenched: The attenuation at the saturated level $\alpha_s$ is rather independent of the temperature and, furthermore, it almost coincides with the minimum attenuation in the temperature dependence.

The characteristic parameters, $\alpha_0$, $\alpha_p$, $\alpha_s$, $H_p$, and $H_s$, which specifies the magnetic field dependences, are defined in Fig. 5. From the temperature dependences which are found in the magnetic field dependence characteristics, the following terms are noted:

($T1$) The magnetic field $H_p$ which gives the maximum attenuation shifts toward lower mag-

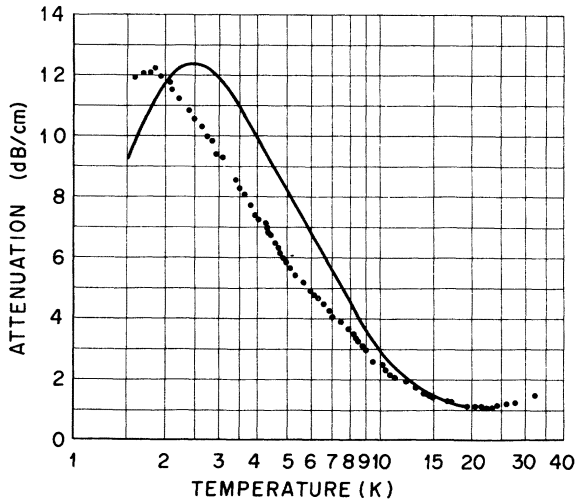


FIG. 3. Temperature dependence of the attenuation of 400-MHz fast transverse waves propagating in the [1$\bar{1}$0] direction in Si17*LD*. In the measurement, a ZnO-piezoelectric film was used as a transducer. The solid curve is the calculated one with $\Delta_0=3.0$ K, $\sigma=2.0$ K, and $\beta=0.11$ (see Sec. III B).

netic field with decreasing temperature, regardless of the magnitude of the attenuation at $H = 0$.

($T2$) The amount of the increment in the attenuation $(\alpha_p - \alpha_0)$ increases with decreasing temperature.

Table II lists the values of the characteristic parameters at 4.23 K to compare the magnetic field dependence in several samples. Since the attenuation is expected to be proportional to $f^2$ and $N_a$ ($f$ is the frequency of the ultrasonic wave) as

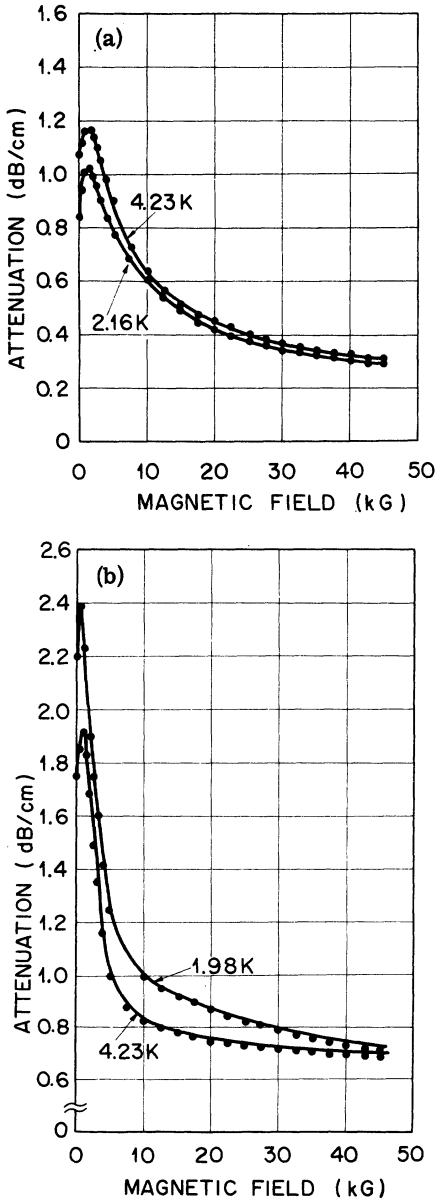


FIG. 4. Magnetic field dependences of the attenuation of 585-MHz fast transverse waves propagating in the [1$\bar{1}$0] direction in (a) Si16*LD* and (b) Si16*HD* at two temperatures. The magnetic field was applied in the [111] direction.

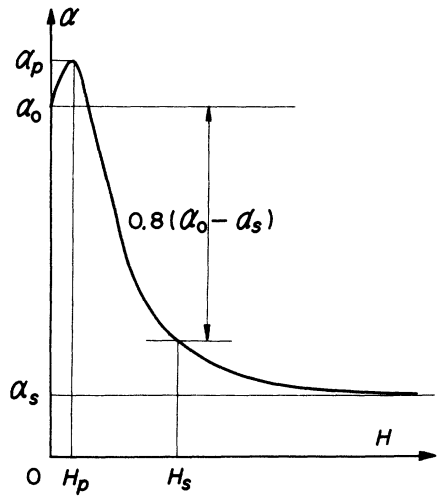


FIG. 5. Definition of the parameters which characterize the magnetic field dependence. The values for several samples are listed in Table II.

will be shown later [Eq. (3)], the values of $\alpha_p - \alpha_0$ and $\alpha_0 - \alpha_s$ are divided by $f^2N_a$ to compare the coupling of waves at various $f$ and $N_a$ [strictly speaking, however, the attenuation also depends on $f$ through Lorentzian terms in Eqs. (4) and (4′)]. In the same table the observation in samples with boron content of $2\times10^{18}$ cm$^{-3}$ (Si18), which belongs to the *intermediate concentration*, is also summarized by quoting from Ref. 19. This is different from the samples belonging to the low concentration region, since the attenuation decreases monotonously with increasing magnetic field.

The effect of the quartz-plate transducer upon the attenuations becomes smaller as the acceptor concentration increases as described before[13] and the properties of Si17*LD* and Si18 are represented rather well by Si17*LDQ* and Si18*Q*, respectively. On the other hand, to indicate the effect of the stress due to the quartz plate, the magnetic field dependences are also summarized in the columns headed by Si16*LDQ* and Si16*HDQ*. In Table II the following points are remarked:

($H1$) The increment of the attenuation $(\alpha_p - \alpha_0)/f^2N_a$, decreases as increasing $N_a$ and it becomes zero in Si18*Q*.

($H2$) The amount of the excess attenuation $(\alpha_0 - \alpha_s)/f^2N_a$ at 4.23 K is of the same order.

($H3$) The maximum and the saturation in the attenuation in Si16*HD* appear at lower magnetic field than in Si16*LD*. The tendency is consistent with the change in both $H_p$ and $H_s$ of Si16*LDQ* (toward lower values from that of Si16*LD*). This also supports that the stress induced by the dislocation resembles that by the quartz plate.

($H4$) Though the effects of both the dislocation

TABLE II. Values of the parameters which characterize the magnetic field dependences of the attenuation at 4.23 K. The letter $Q$ added at the end of the name of the samples indicates that the measurements were performed with quartz-plate transducers.

| | Si16*LD* | Si16*HD* | Si17*LDQ*[a] | Si18*Q*[b] | Si16*LDQ* | Si16*HDQ* |
|---|---|---|---|---|---|---|
| $f$ (MHz) | 585 | 585 | 335 | 156 | 585 | 585 |
| $\alpha_p-\alpha_0$ (dB/cm) | 0.17 | 0.17 | 0.05 | 0. | 0.12 | 0.16 |
| $\alpha_0-\alpha_s$ (dB/cm) | 0.59 | 1.09 | 4.8 | 1.85 | 1.05 | 1.6 |
| $H_p$ (kG) | 1.4 | 0.5 | 1.1 | - | 0.9 | 0.6 |
| $H_s$ (kG) | 27. | 8. | 22. | 28. | 20. | 13. |
| $\frac{\alpha_p-\alpha_0}{f^2N_a}$ $(10^{-23}\frac{\text{dB cm}^2}{\text{MHz}^2})$ | 1.0 | 1.1 | 0.097 | 0. | 0.7 | 1.0 |
| $\frac{\alpha_0-\alpha_s}{f^2N_a}$ $(10^{-23}\frac{\text{dB cm}^2}{\text{MHz}^2})$ | 3.5 | 6.9 | 9.3 | 3.8 | 6.3 | 10.2 |

[a]Reference 13. [b]Reference 19.

and the bonded quartz plate change the excess attenuation toward the same direction (lower $H_p$, lower $H_s$), the combination of the two (realized in Si16*HDQ*) does not enhance the effect.

## III. DISCUSSION

### A. Interaction of Acceptor Holes with Ultrasonic Waves

The ground state of acceptor holes in boron-doped Si has a fourfold degenerate structure due to the tetrahedral symmetry of their environments.[11] The quartet is, however, more or less split into a pair of Kramers doublets because of the presence of the internal stresses in the crystal. Suzuki and Mikoshiba[9] presented a theory to explain the temperature dependence of the excess attenuation in *lightly doped* $p$-Si, in which holes are bound to the acceptors at low temperatures, on the basis of the effective-mass approximation and the assumption of the presence of the randomly distributed local stresses. Since we consider the experimental results on the basis of the theory, it is briefly described here.

They assume that the four levels of the ground state are identified in terms of the atomic $J=\frac{3}{2}$ states and the envelopes of the wave functions are represented by isotropic ($s$-like) variation radial functions. In order to calculate the stress splitting among the states and the matrix elements for the transition of the holes, the following acceptor-hole-lattice Hamiltonian[20] is used:

$$H_{h\text{-}l}=\tfrac{2}{3}D_u^a[(J_x^2-\tfrac{1}{3}J^2)e_{xx}+\text{c.p.}] + \tfrac{1}{3}D_u^{a'}[(J_xJ_y+J_yJ_x)e_{xy}+\text{c.p.}], \quad (1)$$

where $J_i$ is the $i$th component of the angular momentum operator for $J=\frac{3}{2}$, $e_{ij}$ is the conventional strain component, c.p. denotes the cyclic permutation with respect to the indices $x$, $y$, $z$, and $D_u^a$ and $D_u^{a'}$ are the deformation potential parameters.

To perform the calculation in an analytically tractable way, the internal stresses are represented by the normal stresses in the [111] and its equivalent directions, whose magnitude is distributed in the Gaussian/Lorentzian. By taking account of the Raman (two-thermal-phonon) process[21] as well as the direct (one-phonon) process to consider the level broadening, Suzuki and Mikoshiba obtained the formulas for the ultrasonic attenuation $\alpha$ as given below:

$$\alpha=\int_{-\infty}^{\infty}\alpha(\Delta)g(\Delta)d\Delta, \quad (2)$$

$$\alpha(\Delta)=\frac{N_a\hbar\omega^2}{\rho v^3}(\tfrac{2}{3}D_u^{a'})^2[\alpha_1(\Delta)+\alpha_2(\Delta)], \quad (3)$$

$$\alpha_1(\Delta)=\frac{\beta_1}{8kT}\left(N_1\frac{2\Gamma_1}{\hbar^2\omega^2+4\Gamma_1^2}+N_2\frac{2\Gamma_2}{\hbar^2\omega^2+4\Gamma_2^2}\right), \quad (4)$$

$$\alpha_2(\Delta)=\frac{\beta_2}{2kT}\left(N_2\frac{\Gamma_1+\Gamma_2}{(\Delta-\hbar\omega)^2+(\Gamma_1+\Gamma_2)^2} + N_1\frac{\Gamma_1+\Gamma_2}{(\Delta+\hbar\omega)^2+(\Gamma_1+\Gamma_2)^2}\right), \quad (4')$$

$$N_1=(1+e^{\Delta/kT})^{-1}, \quad (5)$$

$$N_2=(1+e^{-\Delta/kT})^{-1}, \quad (5')$$

$$\Delta=\tfrac{2}{3}D_u^{a'}s_{44}X, \quad (6)$$

tential constants at the acceptors, $D_u^a$ and $D_u^{a'}$, become equal to those at the band edges, $D_u$ and $D_u'$, where $\omega$ and $v$ are the angular frequency and the velocity of the ultrasonic wave, respectively, $\rho$ the crystal density, $T$ the temperature, $\Delta$ the energy splitting between the doublets, $s_{44}$ the elastic shear modulus, $X$ the stress, $g(\Delta)$ the distribution function, and $\beta_1$ and $\beta_2$ the reduction factors ($0<\beta_1, \beta_2<1$) which are required because the stress

in the ⟨111⟩ direction gives larger contribution to the attenuation than that in the other direction, for instance, the ⟨100⟩ direction. $\Gamma_1$ and $\Gamma_2$ are the level widths which are represented by the following forms:

$$\Gamma_n = \Gamma_{dn} + \Gamma_{Rn} \quad (n = 1, 2) \ , \tag{7}$$

$$\Gamma_{d1} = \Gamma_0 (1 - e^{-\Delta/kT})^{-1} \ , \tag{8}$$

$$\Gamma_{d2} = \Gamma_0 (e^{\Delta/kT} - 1)^{-1} \ , \tag{8'}$$

$$\Gamma_0 = \frac{2(1+D^2)}{45\pi\rho} \left(\frac{\Delta}{\hbar}\right)^3 D_u^{a'2} G(\Delta) \ , \tag{9}$$

$$\Gamma_{R1} \simeq \Gamma_{R2} \simeq \frac{(1+D^2)(2D_u^{a'}/3)^4}{25\pi^3\rho\hbar^6} (kT)^5 \times \int_0^\infty \frac{x^4 e^x}{(e^x - 1)^2} G^2(xkT)\, dx \ , \tag{10}$$

$$G(\epsilon) = v_1^{-5} f^2\left(\frac{\epsilon}{\hbar w_1}\right) + \tfrac{3}{2} v_2^{-5} f^2\left(\frac{\epsilon}{\hbar v_2}\right) \ , \tag{11}$$

$$f(k) = [1 + (a^* k/2)^2]^{-2} \ , \tag{12}$$

$$D = D_u^a / D_u^{a'} \ , \tag{13}$$

where $a^*$ is the effective Bohr radius of the acceptors, and $v_1$ and $v_2$ are the velocities of the longitudinal and the transverse modes in an isotropic approximation, [22] respectively.

### B. Temperature Dependence in the Dislocation-Free Sample

To perform numerical calculations, we adopt here the deformation potential constants determined by heat-pulse experiments[23] for two reasons. First, they are the values obtained by the measurement on acceptor holes (most of the reported deformation potential constants in $p$-Si are relevant to the valence-band holes[23]). Second, the analysis of the heat-pulse data stands basically on the same principle in the evaluation of the coupling between holes and lattice.

Since it is assumed that the envelope functions consist solely of $s$-like parts, the deformation potential constants at the acceptors, $D_u^a$ and $D_u^{a'}$, become equal to those at the band edges, $D_u$ and $D_u'$, respectively. [20] For the values of $D_u$ and $D_u'$, however, the heat-pulse experiments have offered the different values relevant to either dynamic stresses (thermal phonons) or static stresses. (The "dynamic" and the "static" are discriminated with respect to the relation between the wavelength and the effective Bohr radius of the impurities.) In the present problem, the coupling between the ultrasonic waves and the acceptor holes is calculated with the values for the static stresses, since the wavelength is much longer than the effective Bohr radius ($a^* = 13.6$ Å). On the other hand, for the relaxation of the thermal phonons which determines the level width, the values for the dynamic stresses are applied. Thus, we use the deformation potential constants of $D_u^a = 3.8$ eV and $D_u^{a'} = 6.5$ eV for Eqs. (3) and (6), and $D_u^a = 2.7$ eV and $D_u^{a'} = 4.9$ eV for Eqs. (9) and (10).

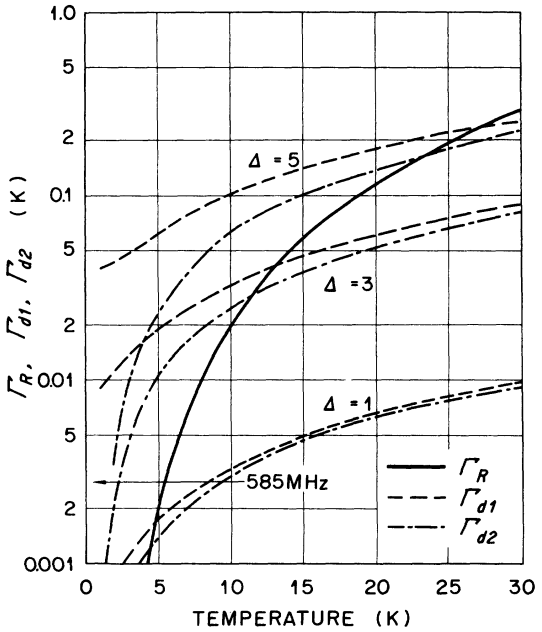


FIG. 6. Temperature dependences of the calculated $\Gamma_{Rn} = \Gamma_R$ ($n = 1, 2$), $\Gamma_{d1}$, and $\Gamma_{d2}$ as functions of the splitting $\Delta$. The values are expressed in units of degrees Kelvin. The arrow mark indicates the temperature corresponding to 585 MHz.

Now, let us check the properties of the formulas on the attenuation [Eqs. (2)–(13)]. To do so, we consider first the attenuation under a uniform stress to make it easier to follow how the stress works in the model, though it is necessary to consider the randomly distributed stress as the internal stress to compare with experiment. The temperature dependences of $\Gamma_{Rn}$ and $\Gamma_{dn}$ ($n = 1, 2$) are shown in Fig. 6, where the stress is expressed in terms of the splitting $\Delta$ in the unit of degrees Kelvin. In Fig. 7 are shown the temperature dependences of the calculated attenuation for the 585-MHz fast transverse waves propagating in the $[1\bar{1}0]$ direction in the sample with $N_a = 4.6 \times 10^{16}$ cm$^{-3}$; here, the following values are used: $\rho = 2.33$ g/cm$^3$, $v = 5.86 \times 10^5$ cm/sec, $v_1 = 9.33 \times 10^5$ cm/sec, $v_2 = 5.42 \times 10^5$ cm/sec, $s_{44} = 1.26 \times 10^{-12}$ cm$^2$/dyn, $\beta_1 = \beta_2 = 1$.

The temperature-dependent parts of Eqs. (4) and (4') consist of the products of $1/T$, $N_1$ ($N_2$), and the Lorentzian-type function including $\Gamma_1$ and $\Gamma_2$; the Lorentzian gives a maximum value when the two squared terms in the denominator become equal. When $\Delta$ is less than 0.5 K, except for $\Delta = \hbar\omega$, the dominant contribution to $\Gamma_1$ and $\Gamma_2$ comes from $\Gamma_{R1}$ and $\Gamma_{R2}$. Thus, $\Gamma_1$ and $\Gamma_2$ at

5.5 K become equal to the energy corresponding to 585 MHz, as shown in Fig. 6. Since $\alpha_1$ includes the terms $N_1$, $N_2$, and $1/T$, in addition to the Lorentzian, the resultant temperature dependence shows the maximum around 8 K, while $\alpha_2$ shows the same temperature dependence if $\Delta \ll \hbar\omega$ (if $\Delta \gg \hbar\omega$, $\alpha_2$ is negligible compared with $\alpha_1$). At $\Delta = \hbar\omega$, however, $\alpha_2$ decreases with increasing the temperature and the contribution of $\alpha_2$ becomes bigger than that of $\alpha_1$.

As $\Delta$ is increased, the contribution of $\Gamma_{d1}$ and $\Gamma_{d2}$ dominates (Fig. 6). Then, the attenuation in the low temperature increases and the maximum in the temperature dependence shifts toward lower temperature. When $\Gamma_{d1}$, $\Gamma_{d2} \gg \hbar\omega$, the temperature dependence of $\alpha_1$ is given by

$$\frac{1}{T}\left(\frac{N_1}{\Gamma_{d1}} + \frac{N_2}{\Gamma_{d2}}\right) = \frac{2}{\Gamma_0 T} \tanh\left(\frac{\Delta}{2kT}\right) \cosh\left(\frac{\Delta}{kT}\right) , \tag{14}$$

which decreases with increasing $T$. On the other hand, since $\Delta \gg T_{d1}$, $\Gamma_{d2}$, and $\hbar\omega$, below 30 K (Fig. 6), the temperature dependence of $\alpha_2$ is given by

$$\frac{1}{T}(\Gamma_{d1} + \Gamma_{d2}) = \frac{\Gamma_0}{T} \coth\left(\frac{\Delta}{2kT}\right) , \tag{15}$$

which decreases with increasing $T$ when $\Delta > kT$. In this limit, however, the absolute value of $\alpha_2$ is much smaller than that of $\alpha_1$, because of the large denominator in the Lorentzian-type function due to $\Delta$.

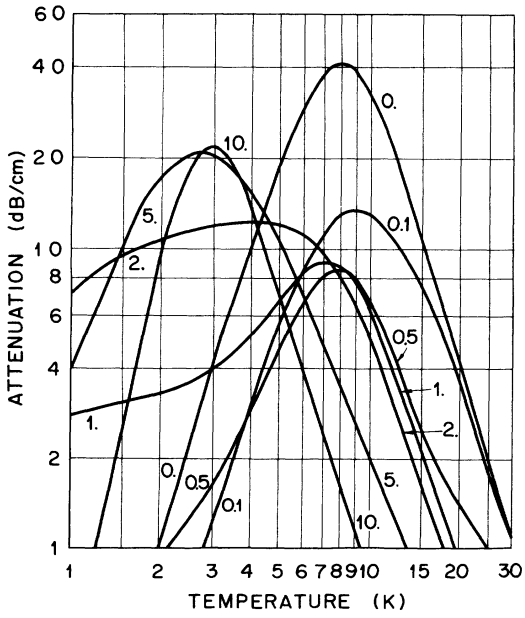


FIG. 7. Temperature dependences of the calculated attenuation at 585 MHz for $N_a = 4.6 \times 10^{16}$ cm$^{-3}$ under uniform stresses. The figures given to the curves represent the splitting $\Delta$ by the internal stress in units of degrees Kelvin.

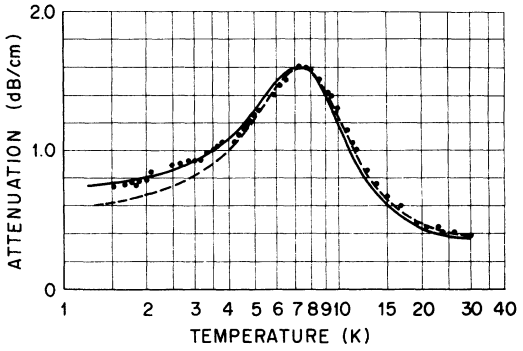


FIG. 8. Comparison of the calculated curves with the experimental result in Si16*LD*. The solid curve is obtained by taking $\Delta_0 = 1.0$ K, $\sigma = 0.3$ K, and $\beta = 0.14$, while the broken curve is obtained by $\Delta_0 = 0.8$ K, $\sigma = 0.3$ K, and $\beta = 0.14$.

The effect of the magnitude of $D_u^a$ and $D_u^{a'}$ is described as follows: If we take larger values for them, the absolute value of the attenuation increases (through the static deformation potential constants) and the peaks shift toward low-temperature side (through the dynamic constants); for example, with dynamic $D_u^a = 3.15$ eV and $D_u^{a'} = 6.3$ eV in Eqs. (9) and (10), the peaks at $\Delta = 0.1$, 1, and 10 K appear at $T = 6.8$, 5.4, and 2.6 K, respectively.

To fit the calculated to the observed temperature dependence, it is required to take account of the presence of the randomly distributed internal stresses.[9] As the distribution function of the internal stresses, we take the Gaussian distribution function,

$$g(\Delta) = (2\pi)^{-1/2}\sigma^{-1} \exp[-(\Delta - \Delta_0)^2/2\sigma^2] , \tag{16}$$

where $\Delta_0$ is the mean and $\sigma^2$ is the variance, because the local stresses are thought to be distributed inhomogeneously.

A good fitting for Si16*LD* has been searched in the following way: Appropriate $\Delta_0$ and $\sigma^2$ have been selected so that the relative change against the temperature is well fitted and then the reduction factors, $\beta_1$ and $\beta_2$, have been decided by making the maximum value near 8 K accord with that calculated on the assumption of $\beta_1 = \beta_2$. In this procedure, the zero level of the excess attenuation has been taken at the saturated level under the strong magnetic field, where it is thought that the excess attenuation due to the acceptor holes is quenched. In Fig. 8 one of the best fits is shown by the solid curve with $\Delta_0 = 1.0$ K, $\sigma = 0.3$ K, and $\beta_1 = \beta_2 = 0.14$. In the same figure, the broken curve obtained by setting $\Delta_0 = 0.8$ K, $\sigma = 0.3$ K, and $\beta_1 = \beta_2 = 0.14$ is also shown to illustrate how the distribution affects the calculation. In these calculations the contribution of $\alpha_1$ dominates.

In Fig. 3 one of the best fitted calculated curves for Si17*LD* is shown. In this case the reduction factors are taken so that both attenuations at 2 K and at 20 K coincide with the measured. The general trend of the results is the appearance of a maximum around 2.5 K and the agreement with the experimental result is not so good as for Si16*LD*. The parameters used for the calculated curve in Fig. 3 are $\Delta_0 = 3.0$ K, $\sigma = 2.0$ K, and $\beta_1 = \beta_2 = 0.11$. In this case also the contribution of $\alpha_1$ dominates.

### C. Dislocation Density Dependence

In the diamond-type lattice, the 60° dislocations which have $(\frac{1}{2}a)\langle 110\rangle$ Burgers vectors ($a$ is the lattice parameter) and $\{111\}$ glide planes are easily found. There are also various types of dislocations, whose angles between Burgers vectors and dislocation axes are distributed from 0° (screw dislocations) to 90° (edge dislocations).[24]

It is believed that the dislocation modifies the acceptor states by introducing mechanical stresses which break the tetrahedral symmetry. The calculation of the stress field around the dislocation, however, is laborious except for a few limited cases; the screw or the edge dislocations in an elastically isotropic media. For the screw dislocations the stresses are expressed in terms of shear stresses, while for the edge dislocations in terms of the combination of normal and shear stresses. It is known that the stress and the strain at moderate and large distances from the dislocation axis are inversely proportional to the radial distance $r$ from the axis.[24]

To consider the effect of the dislocations, we take first a simple model by assuming that the acceptors are distributed uniformly and by neglecting the correlation among the impurities. It is also assumed that the stresses around the dislocations are represented by the stresses along the $\langle 111\rangle$ direction, to take advantage of the formulation in Sec. III A, whose magnitude is given by

$$X = \begin{cases} C/r, & r > r_0 \\ C/r_0, & r < r_0 \end{cases} \tag{17}$$

where $C$ is a constant and $r_0$, which is of the order of several lattice spacings, is introduced to suppress the divergence in $X$ at a point close to the dislocation core. By introducing the cutoff radial distance $r_d$ with the relation,

$$\pi r_d^2 D_d = 1 , \tag{18}$$

the averaged attenuation around the dislocation is given by

$$\alpha_d = \int_{r_0}^{r_d} \alpha(\Delta) 2\pi r dr / \pi r_d^2 \tag{19}$$

($r_d$ is interpreted as the average spacing among the dislocations which are uniformly distributed).

By taking an appropriate value for $C$, temperature dependences which show increases with decreasing the temperature below 3 K are obtained. In Fig. 9 are shown the calculated temperature dependences after Eq. (19) by adopting the following values: $C = 1.32\times10^2$ dyn/cm$^2$ (curve $A$), $1.0\times10^2$ dyn/cm$^2$ (curve $B$), and $6.5\times10$ dyn/cm$^2$ (curve $C$) at $D_d = 2\times10^4$ cm$^{-2}$ corresponding to Si16*HD*. It is remarked that, according to the analysis of the numerical calculation, the temperature dependence below 4 K is attributed to the contribution of the stress region where $\Delta \simeq \hbar\omega$ (resonance absorption of the ultrasonic waves) is satisfied. The temperature dependence for the case of $D_d = 2\times10^2$ cm$^{-2}$ at $C = 1.0\times10^2$ dyn/cm$^2$ is shown by curve $D$ in Fig. 9. The remarkable decrease in the increment of the curve $D$ is consistent with the observation in Si16*MD*, in which almost no dislocation effect is observed. The absolute values of the attenuations in Fig. 9, however, are too large to adjust with the reduction factors described in Sec. III B. The big attenuations are attributed to the resonance absorption. What should be noted here is that the value of the relevant $\Delta$ ($= 2.8\times10^{-2}$ K) is much smaller than the splitting associated with the interactions between the impurities as described in Sec. III B. Therefore it is not reasonable to neglect the presence of the splittings due to the correlation among the impurities.

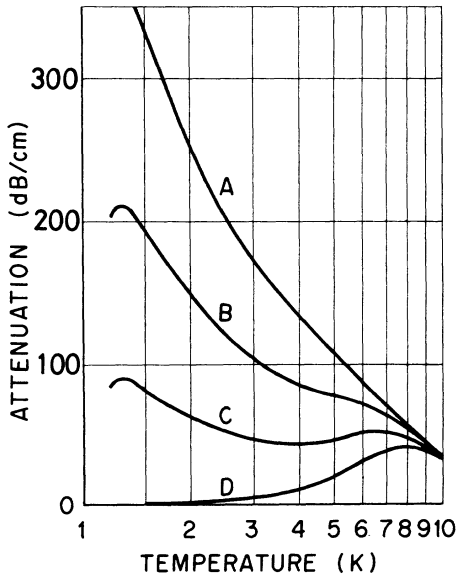


FIG. 9. Temperature dependences of the attenuation at 585 MHz in the sample with dislocations. Curves $A$, $B$, and $C$ are obtained by taking $C = 1.3\times10^2$ dyn/cm$^2$, $1.0\times10^2$ dyn/cm$^2$, and $6.5\times10$ dyn/cm$^2$, respectively, for the sample with the dislocation density of $2\times10^4$ cm$^{-2}$. Curve $D$ is obtained by taking $C = 1.0\times10^2$ dyn/cm$^2$ for the sample with the dislocation density of $2\times10^2$ cm$^{-2}$.

On the basis of the formulation described in Sec. III A, the increase in the attenuation as decreasing temperature below 3 K is realized just by the resonance absorption (Sec. III B). Therefore, if it is shown that the presence of higher dislocation density in addition to the impurities permits the formation of the splittings of $\Delta \simeq \hbar\omega$ in higher probability, the presence of the specific temperature dependence as in Si16*HD* is understood in the framework of the present theory.

Let us consider that the splittings due to the dislocations $\Delta_d$ and due to the interactions among the impurities $\Delta_i$ are distributed independently. Then the distribution of $\Delta = \Delta_d + \Delta_i$ is represented by the following probability density $p(\Delta)$:

$$p(\Delta) = \int_{-\infty}^{\infty} p_i(\Delta - \Delta_d) p_d(\Delta_d) d\Delta_d , \qquad (20)$$

where $p_i(\Delta_i)$ and $p_d(\Delta_d)$ are the probability densities for $\Delta_i$ and $\Delta_d$, respectively. Since $\hbar\omega \ll |\Delta_0|$ is satisfied, under the condition of $\Delta_d > 0$ one obtains

$$p(\hbar\omega) \simeq (2\pi\sigma^2)^{-1/2} \Delta_{dd}^2 \times \int_{\Delta_{dd}}^{\Delta_{d0}} \exp[-(\Delta_d + \Delta_0)^2/2\sigma^2](1/\Delta_d^3) d\Delta_d , \qquad (21)$$

where $\Delta_{d0}$ and $\Delta_{dd}$ are the splittings at $r = r_0$ and $r = r_d$ in the absence of $\Delta_i$, respectively. (Contributions from $\Delta_d > \Delta_{d0}$ are negligible.) Equation (21) indicates that $p(\hbar\omega)$ is a function of $\Delta_{dd}$, in other words a function of $D_d$. If both $\Delta_d$ and $\Delta_0$ have the same sign, Eq. (21) is a monotonically decreasing function of $\Delta_{dd}$, which is not appropriate for the present problem, because with this function the sample with lower $D_d$ has a bigger contribution to the resonance absorption in contrast with the observations. On the other hand, if $\Delta_d$ and $\Delta_0$ have different signs, the $\Delta_{dd}$ dependence of $p(\hbar\omega)$ becomes as shown in Fig. 10, which is obtained under the condition of $\Delta_0 = 1.0$ K, $\sigma = 0.3$ K, $\Delta_{d0} = \infty$. The $p(\hbar\omega)$ decreases as decreasing $\Delta_{dd}$ under $\Delta_{dd} < 0.7$ K in this case. If we take the value of $C \cong 10^3$ dyn/cm$^2$, which is not an abnormal value,[25] the $\Delta_{dd}$ becomes 0.12 K at $D_d = 2.0 \times 10^4$ cm$^{-2}$, and the probability density at $\Delta = \hbar\omega$ decreases with $D_d$ (hence $\Delta_{dd}$), which is preferable to explain the experiment.

Now, it is worthwhile to give light on the assumption that the internal stresses are represented by the normal stresses in the ⟨111⟩ directions in the present formalism. As is well known, to describe a given stress, three principal normal stresses are required[26]: This is easily understood if it is recalled that the symmetrical second-rank tensor is equivalent to a quartic form, which requires three principal components. Thus, the representation of the stresses around the dislocation in terms of the normal stresses is not a good approximation and this fact is responsible for the incompleteness of the present theory.

As a conclusion of this section, it can be said that an appropriate combination of the two types of the internal stresses (due to the dislocations and the impurities) is considered to increase the probability of the formation of the level splitting, $\Delta = \hbar\omega$, and thereby the increment below 3 K in Si16*HD* is ascribed to the resonance absorption of the ultrasonic waves.

### D. Effects of Boron and Oxygen Content

As pointed out in Sec. II A, the temperature dependences in the samples with boron content of $4.6$–$4.9 \times 10^{16}$ cm$^{-3}$ are characterized by the peak near 8 K, which is explained by the presence of the internal stresses of $\Delta_0 = 1.0$ K and $\sigma = 0.3$ K in terms of the aforementioned model. On the other hand, for Si17*LD*, the best fit is obtained by taking $\Delta_0 = 3.0$ K and $\sigma = 2.0$ K. Thus, the specific difference between Si16*LD* and Si17*LD* is attributable to the difference in the distribution of the internal stresses associated with the correlation among the impurities. Furthermore, it is noted that the specific attenuation (the peak near 8 K in Si16*LD*) is remarkably modified neither by the presence of the dislocations nor by the oxygen content.

It is known that there are considerable concentrations of electrically inactive elements in Si, such as oxygen and carbon.[16] The content of oxygen in a pulled crystal is reported to be $10^{17}$ cm$^{-3}$ or more. Furthermore, it is reported that the oxygen stays mainly at interstitial sites while the boron stays at substitutional sites. Based on these facts, it is expected that, as point imperfections, the oxygen may produce stronger mechanical stresses than the boron on an average. Nevertheless, the effect of the oxygen is negligible com-

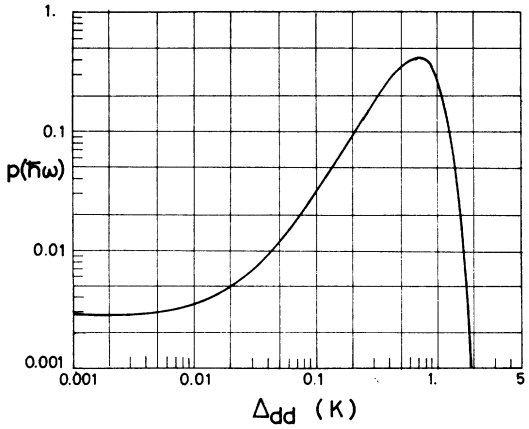


FIG. 10. Calculated $p(\hbar\omega)$ at $\hbar\omega = 2.8 \times 10^{-2}$ K (585 MHz) as a function of $\Delta_{dd}$ under the condition of $\Delta_0 = 1.0$ K and $\sigma = 0.3$ K, which corresponds to Si16*LD*.

pared to that of the boron, in contrast to the thermal conductivity.[27]

Now we consider that for the thermal phonons the oxygen atoms themselves act as scatterers, while for the ultrasonic waves, which have very long wavelength, the oxygens do not act as strong scatterers. The presence of oxygen may modify the attenuation by modulating the acceptor states through affecting the local mechanical stresses. It should be remarked, however, that the stress distribution around the point imperfections in crystals is localized because the stress decreases proportionally to the third power of the distance from the defects,[24] and, moreover, as the diamond lattice is not densely packed, the strains associated with the point imperfections are small. Since the probability density of finding the nearest neighbor at the distance $R$ is given by

$$p(R) = 4\pi N R^2 e^{-(4/3)\pi N R^3}, \tag{22}$$

where $N$ is the content of the impurity atoms, the probability of the encounter between two atoms even with the separation of several times of the interatomic distance (2.4 Å) is low.[28] Thus, it is considered that the stresses induced by uniformly distributed point imperfections in Si cannot offer the considerable local stresses which are described in Sec. III B.

One of the ways to interpret the considerable stresses among the boron impurities is to take account of the possibility of the preferential aggregation or clustering of the atoms, but such clustering has not been reported in this kind of low concentration of boron in Si. The other way is to pay attention to the extent of the acceptor wave function. Though it is reported that the effective Bohr radius of boron in Si is 13.6 Å, the tail of the wave function spreads to further extent.[20] Since the borons are randomly distributed, the interactions at the tails break the tetrahedral symmetry of an acceptor state and lift the degeneracy of its ground states. In the higher concentration, modification of the ground states is stronger because of the closer interactions among the borons. Thus, it is reasonable to consider that the inherent internal stresses are ascribed to the electronic correlation among the acceptors instead of the mechanical stresses through lattice deformations.

According to Suzuki and Mikoshiba,[29] the splitting by the formation of the molecular-ion type combinations of the borons, which is probable in the presence of the compensating impurities, is given by the following relation:

$$\Delta = (2e^2/\kappa R)[(2/3)(R/a^*)^2 - 1]e^{-R/a^*}, \tag{23}$$

where $R$ is the spacing between two atoms forming a pair and $\kappa$ is the dielectric constant. By taking account of the probability density for $R$ [by Eq. (22)], the temperature dependences of the attenuation for $N = N_a = 5\times10^{16}$ cm$^{-3}$ and $N_a = 5\times10^{17}$ cm$^{-3}$ are obtained as shown in Fig. 11 by the solid and the broken curves, respectively, under the assumption of full compensation. One can get the attenuation at the intermediate compensation by simply multiplying the compensation ratio. The peaks in the calculated curves appear at different temperatures from the observation. Therefore, the correlation between the acceptors cannot be explained in terms of the molecular-ion model.

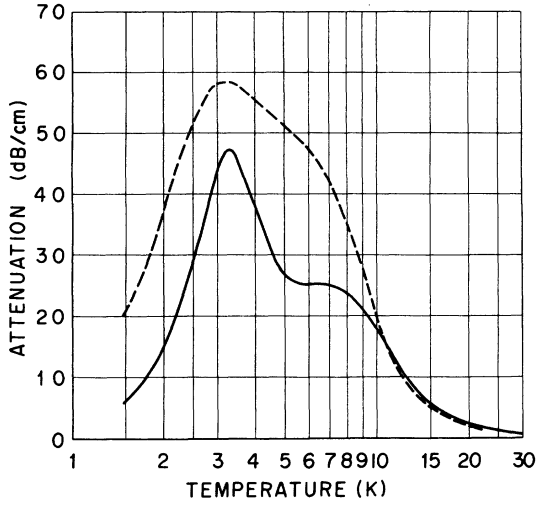


FIG. 11. Temperature dependences of the attenuation due to molecular-ion centers. The solid curve is for $N_a = 5\times10^{16}$ cm$^{-3}$ at 585 MHz and the broken curve is for $N_a = 5\times10^{17}$ cm$^{-3}$ at 400 MHz.

### E. Magnetic Field Dependance

In the low-magnetic-field region, where the splitting due to the internal stresses is much larger than the Zeeman splitting, the attenuation is calculated by regarding the Zeeman effect as a perturbation to the system. On the other hand, in the strong-field limit, the direction of the quantization for the Hamiltonian should be taken in the direction of the external magnetic field. These calculations have given a semiquantitative explanation of the magnetic field dependences.[13] The attenuation shows a small increment at low magnetic field due to the resonance transitions of the acceptor holes among the randomly distributed splitting states and decreases sharply down to the levels where the attenuation due to the hole-lattice coupling is quenched because of the large Zeeman splitting.[13,19]

As described in Sec. II B, the presence of the dislocations reduces the saturation field $H_s$ [see Fig. 5 and ($H3$) in Sec. II B]. To discuss this be-

havior, we write down here the attenuation formula in the presence of the strong magnetic field, which is obtained by taking the direction of the quantization along that of the external magnetic field (in our case this corresponds to the [111] direction). It is assumed as in Sec. III A that the relevant states of the acceptors are described by the magnetic quantum numbers and the local stresses are represented by the normal stresses along the [111] direction. Then, in the presence of both the strong magnetic field $H$ in the [111] direction and the splitting due to the local stress $\Delta$, the attenuation of the fast transverse waves propagating in the $[1\bar{1}0]$ direction is given by

$$\alpha(\Delta, H)=\frac{\omega}{\rho v^3}\frac{\hbar\omega}{kT}\sum_{nn'}N_n\left(\tfrac{2}{3}D_u^{a'}\right)^2\left|C_{qt}^{nn'}\right|^2 \times\frac{\Gamma_n}{(\hbar\omega-E_{n'n})^2+\Gamma_n^2}\ , \tag{24}$$

$$\begin{aligned}\Gamma_1&=(2D^2+1)\gamma_1(E_{12})+(D^2+2)\gamma_1(E_{13})\ ,\\ \Gamma_2&=(2D^2+1)\gamma_2(E_{12})+(D^2+2)\gamma_1(E_{24})\ ,\\ \Gamma_3&=(D^2+1)\gamma_2(E_{13})+(2D^2+1)\gamma_1(E_{34})\ ,\\ \Gamma_4&=(D^2+1)\gamma_2(E_{24})+(2D^2+1)\gamma_2(E_{34})\ ,\end{aligned} \tag{25}$$

$$\gamma_1(\Delta)=\frac{2D_u^{a'2}}{135\pi\rho}\left(\frac{\Delta}{\hbar}\right)^3\left[1-\exp\left(-\frac{\Delta}{kT}\right)\right]^{-1}G(\Delta)\ , \tag{26}$$

$$\gamma_2(\Delta)=\frac{2D_u^{a'2}}{135\pi\rho}\left(\frac{\Delta}{\hbar}\right)^3\left[\exp\left(\frac{\Delta}{kT}\right)-1\right]^{-1}G(\Delta)\ ,$$

$$\begin{aligned}E_{12}&=1.01\,\mu_B H+2\Delta\ ,\\ E_{34}&=1.01\,\mu_B H-2\Delta\ ,\\ E_{13}&=2.45\,\mu_B H+2\Delta\ ,\\ E_{24}&=2.45\,\mu_B H-2\Delta\ ,\end{aligned} \tag{27}$$

$$\left|C_{qt}^{nn}\right|^2=0,\quad \left|C_{qt}^{12}\right|^2=\left|C_{qt}^{34}\right|^2=0.25,\quad \left|C_{qt}^{13}\right|^2=\left|C_{qt}^{24}\right|^2=0.5\ , \tag{28}$$

where $\mu_B$ is the Bohr magneton.

Thus, the magnetic field dependence of the attenuation under the presence of the randomly distributed internal stresses (expressed in terms of the Gaussian distribution) is given by

$$\alpha_I(H)=(2\pi\sigma^2)^{-1/2}\int_{-\infty}^{+\infty}\alpha(\Delta_i, H)\times\exp[-(\Delta_i-\Delta_0)^2/2\sigma^2]\,d\Delta_i\ , \tag{29}$$

while in the presence of the dislocations but in the absence of the correlations among the impurities

$$\alpha_D(H)=\int_{r_0}^{r_d}\alpha(\Delta_d, H)\,2\pi r\,dr\ . \tag{30}$$

The calculated $\alpha_I(H)$ and $\alpha_D(H)$ are shown in Fig. 12 as a function of $H$, where the attenuations are normalized with the values at $H=5$ kG. It is shown that $\alpha_D(H)$ decreases more rapidly with $H$ than $\alpha_I(H)$. This is consistent with the observations. The small splittings which contribute to the resonance absorption are disturbed easily by the application of the external magnetic field.

The increment in the attenuation $(\alpha_p-\alpha_0)$ decreases as increasing boron content [$(H1)$ in Sec. II B]. This is explained in the following way: Since the increment is attributed to the resonance transition of holes among the levels which are changed by the external field, if the magnitude of the internal stress is widely distributed, the percentage of the acceptors which satisfy the resonance condition at a given field is limited. Consequently the increment is diminished as a whole.

### F. Limits of Validity of Model

The experimental results are fairly well explained in terms of the acceptor-hole-lattice interactions by taking account of the internal stress distribution. It has been required, however, to use some adjustable parameters to fit the calculated to the experiments. This comes partly from the shortage in the knowledge on the stress distribution, but the adopted simplifications have caused the incompleteness of the model. We conclude this paper by pointing out these problems.

First, we point out the neglect of the $d$-like (anisotropic) terms in the envelope function.[20] It is not serious, however, since the contribution of these parts is less than 7% because of the large

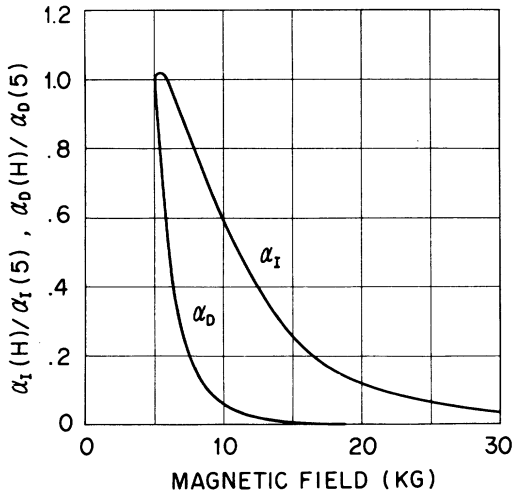


FIG. 12. Magnetic field dependences of the attenuation of 585-MHz fast transverse waves propagating in the $[1\bar{1}0]$ direction. The curves are normalized by the attenuation at $H=5$ kG. The curve $\alpha_I$ is obtained for the sample with the random stresses which are characterized by the Gaussian with $\Delta_0=1.0$ K and $\sigma=0.8$ K. The curve $\alpha_D$ is obtained for the sample with dislocation density of $2\times10^4$ cm$^{-2}$.

spin-orbit splittings in Si.[20] On the other hand, the representation of the local random stresses by the normal stresses in the ⟨111⟩ directions should be noticed, since this is rather unrealistic as mentioned in Sec. III C. Nevertheless, if three nonzero normal stresses are introduced, the acceptor-hole-lattice coupling Hamiltonian in terms of the angular momentum is not useful and there has not been discovered a tractable way to develop theory. The incompleteness in the description of the internal stresses in the model has been compensated by introducing the adjustable parameters $\beta_1$ and $\beta_2$.

Third, it is found that the correlation among the acceptors (its effect is treated as the presence of the internal stresses in this paper) modifies the acceptor states considerably, even at the concentration of $5\times10^{16}$ cm$^{-3}$. The correlation becomes stronger in the higher concentration and the one-acceptor model used here breaks. For instance, a limit of the localized acceptor model is clearly revealed in the magnetic field dependence in Si18, the sample in the intermediate concentration region, where the saturation levels at 4.23 and 3.64 K under the strong magnetic field do not coincide.[19] This is not explained in terms of the localized acceptor model. Generally speaking, however, the attenuation by the interacting impurities is kept unsolved even in $n$-type Si[30] and Ge.[31,32]

ACKNOWLEDGMENTS

The author would like to express his sincere thanks to N. Mikoshiba, K. Suzuki, and T. Iizuka for their helpful discussions. He is also obliged to M. Pomerantz, who gave valuable suggestions. Thanks are extended to T. Abe of Shinetsu Semiconductors Co. for supplying the samples and R. Inaba for the preparation of ZnO films. The support by the members of Solid State Group in ETL is acknowledged.

[1]W. P. Mason and T. B. Bateman, Phys. Rev. **134**, 1386 (1964).
[2]M. Pomerantz, Proc. IEEE **53**, 1438 (1965).
[3]M. Pomerantz, Phys. Rev. B **1**, 4029 (1970).
[4]R. W. Keyes, IBM J. Res. Dev. **5**, 266 (1961).
[5]R. W. Keyes, in *Solid State Physics*, edited by F. Seitz and D. Turnbull (Academic, New York, 1967), Vol. 20, p. 37.
[6]K. Suzuki and N. Mikoshiba, Phys. Lett. **23**, 44 (1966).
[7]P. C. Kwok, Phys. Rev. **149**, 666 (1966).
[8]P. Csavinsky and N. G. Einspruch, Phys. Rev. **132**, 2434 (1963).
[9]K. Suzuki and N. Mikoshiba, Phys. Rev. Lett. **28**, 94 (1972).
[10]H. Hasegawa, Phys. Rev. **129**, 1029 (1963).
[11]W. Kohn, in Ref. 5, Vol. 5, p. 257.
[12]T. Ishiguro, T. A. Fjeldly, and C. Elbaum, Solid State Commun. **10**, 1309 (1972).
[13]T. Ishiguro, K. Suzuki, and N. Mikoshiba, in *Proceedings of the International Conference on the Physics of Semiconductors, Warsaw, 1972* (PWN-Polish Scientific Publishers, Warsaw, 1972), p. 1239. $g(1/2)$ and $g(3/2)$ in Table I should be read as $2g(1/2)$ and $2g(3/2)$, respectively.
[14]M. Pomerantz (private communication). A part of the work is presented in Proceedings 1968 Sendai Symposium on Acousoelectronics, Sendai, Japan, p. 39 (unpublished).
[15]J. C. Irvin, Bell Syst. Tech. J. **41**, 387 (1962).
[16]See for example, W. Kaiser and P. H. Keck, J. Appl. Phys. **28**, 882 (1957).
[17]R. Inaba, T. Ishiguro, and N. Mikoshiba, Jap. J. Appl. Phys. **10**, 1493 (1971).
[18]R. K. Kirby, in *American Institute Physics Handbook*, 2nd ed. (McGraw-Hill, New York, 1963), pp 4–66 and 4–74.
[19]T. Ishiguro and S. Waki, Phys. Lett. A **39**, 85 (1972).
[20]K. Suzuki, M. Okazaki, and H. Hasegawa, J. Phys. Soc. Jap. **19**, 930 (1964).
[21]L. M. Roth, Phys. Rev. **118**, 67 (1960).
[22]F. I. Fedorov, *Theory of Elastic Waves in Crystals* (Plenum, New York, 1968), Chap. 5.
[23]T. A. Fjeldly, T. Ishiguro, and C. Elbaum, Phys. Rev. B **7**, 1392 (1973).
[24]H. G. Van Bueuren, *Imperfections in Crystals* (North-Holland, Amsterdam, 1960), p. 599.
[25]W. T. Read, *Dislocations in Crystals* (McGraw-Hill, New York, 1953), p. 114.
[26]J. F. Nye, *Properties of Crystals* (Clarendon, Oxford, England, 1964), p. 89.
[27]M. G. Holland, in *Proceedings of the International Conference on Physics of Semiconductors, Prague, 1960* (Academic, New York, 1961), p. 633.
[28]S. Sonder and H. Schweinder, Phys. Rev. **117**, 1216 (1960).
[29]K. Suzuki and N. Mikoshiba, in *Proceedings of the Conference on Phonon Scattering in Solids, Paris, 1972* (La Documentation Francaise, Paris, 1972), p. 125.
[30]M. Dutoit, Phys. Rev. B **3**, 453 (1971).
[31]T. Ishiguro and N. Mikoshiba, in *Proceedings of the International Conference on Physics of Semiconductors, Cambridge, 1970* (NBS, Springfield, Va., 1970), p. 569.
[32]N. Mikoshiba and T. Ishiguro, Phys. Lett. A **36**, 455 (1971).